



# MANFIS–GA Heat Transfer Analysis and Optimization of Fins with Elliptical Perforation

C. Balachandar<sup>1</sup> · S. Arunkumar<sup>1</sup> · R. Madhumitha<sup>1</sup> · M. Venkatesan<sup>1</sup>

Received: 2 June 2017 / Accepted: 9 May 2018 / Published online: 22 May 2018  
© Shiraz University 2018

## Abstract

In the present work, numerical heat transfer analysis of fins with elliptic perforations is performed and a soft computing-based optimization method is proposed for its design. The computational analysis is performed by solving coupled heat and flow transport equations after validating the numerical model with an existing experimental result. A parametric study is done based on the numerical model to examine the effects of fin spacing, fin height, fin perforation major axis, minor axis lengths and the number of perforations. The analyzed model results in an increased heat transfer rate with volume reduction of up to 72% when compared to a rectangular solid fin. But the best heat transfer rate and volume reduction are not achieved for the same set of fin parameters. A multiple response optimization technique needed to arrive at a fin configuration that provides considerable reduction in weight along with an increase in heat transfer is proposed. It is difficult to obtain reasonable approximations using mathematical regressions for such multiple response optimizations as the system response is highly nonlinear. An attempt is made to use multiple output adaptive neuro-fuzzy inference system coupled with genetic algorithm to optimize the parameters of the fins with elliptical perforation considering increased heat transfer and weight reduction. The proposed new optimization algorithm is found to be more effective in determining the optimal parameters when compared to existing regression and soft computing methods for optimization.

**Keywords** Heat fin · Elliptical perforation · MANFIS–GA · Computational analysis · Optimization

## List of symbol

$H$	Convection heat transfer coefficient, $W/(m^{-2} K)$
$A$	Area, $m^2$
$Nu$	Nusselt number
$S$	Fin spacing
$H$	Fin height
$N$	Number of fins
$L$	Fin length
$W$	Fin width
$t$	Fin thickness
$d$	Base plate thickness
$L_p$	Perforation major axis length
$L_{opt}$	Optimized major axis length
$W_p$	Perforation minor axis length
$W_{opt}$	Optimized minor axis length
$N$	Number of perforations
$Ra$	Rayleigh number

$T_w$	Average base plate temperature, °C
$T_a$	Ambient temperature, °C
$T$	Temperature, °C
$\Delta T$	Base-to-ambient temperature diff., °C
$k$	Thermal conductivity, $W/(m K)$
$g$	Gravitational acceleration, $m/s^2$
$\beta$	Volumetric thermal expansion coefficient, $1/K$
$\nu$	Kinematic viscosity, $m^2/s$
$\alpha$	Thermal diffusivity, $m^2/s$

## 1 Introduction

Heat fins are used extensively to decrease the temperature of heated base surfaces. Design of fins with maximum efficiency has been a prime area of research for years. In general, the fin efficiency is increased in two ways. One way is to reduce the mass for a given amount of heat dissipation, and the other is to increase the heat dissipation for a given volume by increasing heat transfer rate. In the very beginning, experimental studies were conducted on fins of various geometries to arrive at an optimal parameter

✉ M. Venkatesan  
mvenkat@mech.sastra.edu

<sup>1</sup> School of Mechanical Engineering, SAstra Deemed University, Thanjavur 613401, India

for augmented heat transfer. Welling and Wooldridge (1965) studied the dependence of heat transfer on vertical fin geometry. They concluded that there exists an optimal fin height for an augmented heat transfer. Leung and Probert (1989) presented non-dimensional correlations based on the experiment on vertical fins on the vertical base plate. An optimal inter-fin separation for improved heat transfer was presented. They also did an experiment on vertical rectangular fins arriving at an optimal separation of fins (Leung et al. 1985). An experiment on the heat exchanger with vertical rectangular fins was conducted to determine ideal values of the vertical fin array's geometrical parameters for achieving maximum heat transfer (Leung and Probert 1987). Güvenç and Yüncü (2001) did an experimental investigation on 15 different fin configurations to arrive at an optimal fin parameter. It was concluded that for the same configuration, vertically oriented setup resulted in improved heat transfer characteristics than the setup with horizontal orientation. Yazicioğlu and Yüncü (2007) experimentally studied the heat transfer characteristics on rectangular fins under natural convection condition. Correlations for arriving at an optimal fin spacing for augmented heat transfer was developed. The literature (Welling and Wooldridge 1965; Leung and Probert 1989; Leung et al. 1985; Leung and Probert 1987; Güvenç and Yüncü 2001; Yazicioğlu and Yüncü 2007; Çakar 2009) reveals that there are few works describing the optimization of fin parameters for rectangular fins. In the present study, the objective is to design fins that enhance heat transfer rate with decreased weight when compared to conventional plate fins.

Earlier, fins of different geometries have been studied to increase the heat transfer characteristics. One way to enhance the heat transfer rate of a heat sink is to introduce perforations in the plate fin. Perforations in fins allow air or convective fluid to pass through them taking away a considerable amount of heat. The applicability of perforated fins was extensively studied (Tari and Mehrtash 2013; Sparrow and Ortiz Carranco 1982; Prasad and Gupta 1998; Kutscher 1994; Souidi and Bontemps 2001; Al-Essa 2012; Akyol and Bilen 2006; Sahin and Demir 2008a, b; Al Essa et al. 2009; Essa and Al-Odat 2009; Al Essa and Al-Widyan 2008; Al Essa and Al-Hussien 2004; Shaeri et al. 2009; Shaeri and Jen 2012; Huang et al. 2015; Dorignac et al. 2005) under various conditions. Souidi and Bontemps (2001) studied countercurrent gas–liquid flow in narrow rectangular channels simulated by plain and perforated fins. Analytical studies were done on different types of perforated fins by Al-Essa (2012). Abdullah et al. (Al Essa et al. 2009; Essa and Al-Odat 2009; Al Essa and Al-Widyan 2008; Al Essa and Al-Hussien 2004) studied the characteristics of the fin with different orientations of perforations. The results were compared with solid fins. It was

concluded that for certain geometry and size of perforation there is augmented heat transfer along with a significant drop in the weight of the fin. Lateral perforated heat fin sinks under forced convection were examined by Shaeri et al. (2009). Shaeri and Jen (2012) studied the heat transfer characteristics of rectangular fin array with rectangular perforations. They numerically investigated the heat transfer characteristic by varying the geometry and number of perforations and concluded that fins with perforations show augmented heat transfer compared to the conventional fins. Typically, in the majority of these cases, the perforation shape was rectangular. The effect of cylindrical perforations was studied by Huang et al. (2015). Based on the numerical investigation, they have fabricated fin array with perforations and experiments were conducted to study the heat transfer characteristics. Levenberg–Marquardt method is used to optimize the diameter of the perforations.

The literature review shows that various fin geometries and fins with perforations have been analyzed and optimized. But there is a need to develop an optimization technique that reduces the need for multiple trial and errors. In the present work, a numerical model and an optimization technique are developed to analyze the heat transfer characteristics in a plate fin kept over a vertical plate and to arrive at an optimal fin geometry. Validation of the developed numerical model is done with experimental results for solid plate fins available in Yazicioğlu and Yüncü (2007). Natural convection heat transfer plays an important role in cooling of molten metals, solar ponds, etc. Thus, the design of heat transfer devices working under free convection is of utmost importance in industrial applications. After validating the developed numerical model for solid fins, the case of elliptically perforated fins is taken up and analyzed. The numerical model is shown in Fig. 1.

ANSYS FLUENT© solver (ANSYS 2008) is used to solve the governing transport and energy equations. Surface-to-surface radiation model is used for radiation. Fins with different perforation dimensions and numbers of perforations are analyzed. It was observed during the numerical analysis that elliptical fins had a better heat transfer rate when compared to solid fins of comparable geometry. Moreover, there is a considerable decrease in weight of the fin as a result of perforations. However, the maximum weight reduction and heat transfer augmentation are obtained for different combinations. Thus, the need to perform a multiobjective optimization study is evident. Typically, multiresponse optimization studies are carried out using evolutionary algorithms (Zimmermann 1978; Chambers 1992; Culliere Th et al. 1995; Balachandar et al. 2015; Wessa 2015). Zimmermann (1978) proposed fuzzy linear programming approach to solve linear programming problems with several objective functions. Culliere et al. (1995) used a combination of fuzzy sets and neural

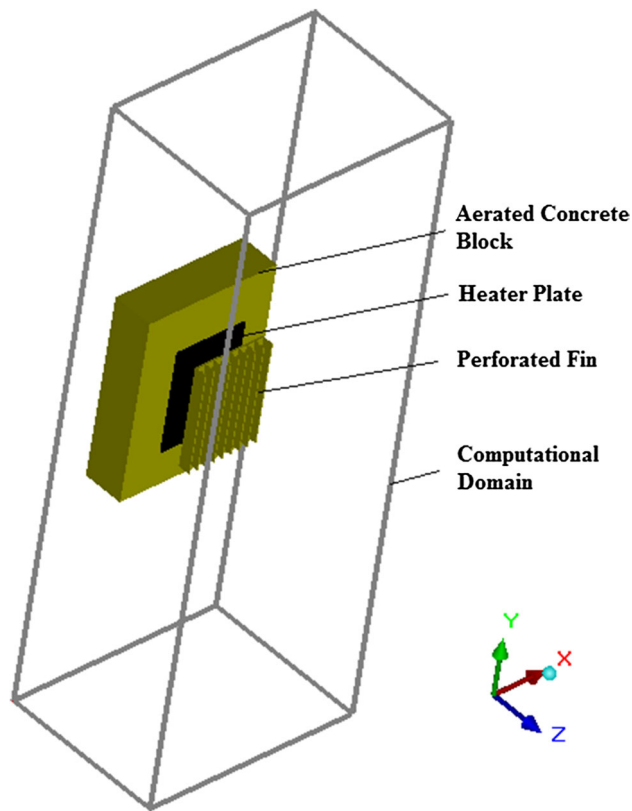


Fig. 1 Setup model

networks for nonlinear systems. Balachandar et al. (2015) used a combination of artificial neural network and genetic algorithm for heat transfer studies. They used this combination to optimize hollow pin fins for an effective heat transfer. Their study involved arriving at a minimum base plate temperature along with weight reduction of the fin. The simulations were fed to train the ANN, and GA was applied on the trained ANN to arrive at an optimal geometry satisfying the two objectives of the study. Optimization algorithms demand a mathematical function that characterizes the objective in terms of parameters. As the present case involves considerable nonlinearity in arriving at the objective function, MANFIS-based prediction coupled with GA is used to arrive at an optimal geometry of fin.

## 2 Numerical Model and Validation

Natural convection in rectangular solid fins by Yazicioğlu and Yüncü (2007) is taken as base work for the present analysis. The model in Çakar (2009) and Tari and Mehrtash (2013) with the aerated concrete block is taken for numerical simulations and for numerical model validation. The model consists of an array of rectangular fins kept over a vertical base plate of dimension  $250 \times 180 \times 5$  mm. This setup is kept over an aerated concrete block of dimension

$340 \times 450 \times 100$  mm. The material properties are mentioned in Table 1. The fin assembly is kept inside a computational domain of dimension of size  $540 \times 1500 \times 400$  mm which is maintained at an initial ambient temperature of  $20$  °C. A standard pressure discretization scheme is used with a second-order momentum equation. The skewness value for the mesh is 0.15. No-slip boundary condition for all the surfaces and contact resistance between solid surfaces are assumed to be zero. Air is taken as an ideal gas at atmospheric pressure and continuity; momentum and thermal energy equations are solved. In the numerical model, convergence criteria for flow is  $1e-3$ . The criteria is  $1e-7$  for energy, turbulent kinetic energy, and turbulent dissipation rate.

### 2.1 Grid Independence Study

The computational domain is shown in Fig. 1. The base plate of the fin is heated with a constant heat source from its bottom side. ANSYS FLUENT © solver is used to obtain a steady-state solution for the governing equation comprised of flow and conduction. Grid independence test is carried out by measuring the average base plate temperature. The number of mesh elements was increased, and the variances in the temperature for successive grid elements were recorded. Grid independence with a variance of less than  $\pm 0.75$  °C is accomplished for a total of  $1.35E+6$  mesh elements. A non-conformal mesh structure with a very fine grid around the cooling assembly and a coarse grid for the rest of the room was used for discretization.

### 2.2 Numerical Model Validation

The experimental setup (Yazicioğlu and Yüncü 2007) is modeled and simulated for a fin length of 250 mm and a fin height of 25 mm. Comparison of the Nusselt number for solid fins with available correlations (Eqs. 1–3) and present numerical model and the experimental results of Yazicioğlu and Yüncü (2007) is tabulated in Table 2. The maximum percentage error in the comparison is 2.65%. The numerical model is designed for laminar heat transfer and periodically checked for the transition from laminar to turbulent.

*McAdams' relation* (McAdams 1954):

$$Nu = 0.59Ra^{1/4}. \quad (1)$$

*Churchill and Chu's first relation* (Churchill and Chu 1975):

$$Nu = \left[ 0.825 + \frac{0.387Ra^{1/6}}{\left[ 1 + (0.492/Pr)^{9/16} \right]^{8/27}} \right]^2. \quad (2)$$

**Table 1** Material properties

Components	Material type	Specific heat (J/kg K)	Conductivity (W/m K)	Emissivity	Roughness (mm)
Concrete block	Aerated concrete	1000	0.15	0.9	2
Heater base plate	Aluminum	900	130	0.2	0.02
Fin array	Aluminum	900	130	0.2	0.02

**Table 2** Validation

$Q_{in}(W)$	$Ra$	Average $Nu$				
		McAdams' relation	Churchill and Chu's first relation	Churchill and Chu's second relation	Comparison with Ref. (Yazicioglu and Yüncü 2007)	Present study
20	4.87E+7	49.26	49.26	43.58	45.59	46.78
30	6.11E+7	52.11	52.63	46.05	48.33	49.42
40	6.88E+7	53.51	54.51	47.62	49.92	50.37

Churchill and Chu's second relation (Churchill and Chu 1975):

$$Nu = 0.68 + \frac{0.67Ra^{1/4}}{\left[1 + (0.492/Pr)^{9/16}\right]^{8/27}} \tag{3}$$

The Rayleigh number ( $Ra$ ) in the above equations is defined based on heat sink length as

$$Ra = \frac{g\beta L^3(T_w - T_a)}{\nu\alpha}$$

### 2.3 Problem Description: Fins with Elliptic Perforations

Natural convection on elliptically perforated fins is analyzed to determine the effect of fin parameters on base plate temperature and Nusselt number. Perforations of elliptic dimensions are introduced along the length of the fin. Heat transfer depends on parameters such as fin spacing ( $S$ ), heat sink length ( $L$ ), fin height ( $H$ ), the number of perforations ( $n_p$ ), perforation major ( $L_p$ ) and minor axis ( $W_p$ ). In this analysis, fin length is kept constant as 250 mm. A 20 W source is used to supply heat load at the base plate in the present work. The governing equations of the problem are as follows:

The mass conservation equation given in Eq. 4 is based on incompressible fluid assumption.

$$\frac{\partial u}{\partial x} + \frac{\partial v}{\partial y} + \frac{\partial w}{\partial z} = 0 \tag{4}$$

Variables  $u, v, w$  are the components of velocity in  $x-, y-$  and  $z$ -directions, respectively. The conservation of

momentum equations in three dimensions are shown in Eq. 5 with a Boussinesq approximation for modeling temperature dependent density.

$$\begin{aligned} u \cdot \frac{\partial u}{\partial x} + v \cdot \frac{\partial u}{\partial y} + w \cdot \frac{\partial u}{\partial z} &= \nu \left( \frac{\partial^2 u}{\partial x^2} + \frac{\partial^2 u}{\partial y^2} + \frac{\partial^2 u}{\partial z^2} \right) + g \cdot \beta \cdot \Delta T \\ u \cdot \frac{\partial v}{\partial x} + v \cdot \frac{\partial v}{\partial y} + w \cdot \frac{\partial v}{\partial z} &= \nu \left( \frac{\partial^2 v}{\partial x^2} + \frac{\partial^2 v}{\partial y^2} + \frac{\partial^2 v}{\partial z^2} \right) + g \cdot \beta \cdot \Delta T \\ u \cdot \frac{\partial w}{\partial x} + v \cdot \frac{\partial w}{\partial y} + w \cdot \frac{\partial w}{\partial z} &= \nu \left( \frac{\partial^2 w}{\partial x^2} + \frac{\partial^2 w}{\partial y^2} + \frac{\partial^2 w}{\partial z^2} \right) + g \cdot \beta \cdot \Delta T \end{aligned} \tag{5}$$

The conservation of energy equation is shown in Eq. 6

$$\begin{aligned} g \cdot Cp \cdot \left( u \cdot \frac{\partial T}{\partial x} + v \cdot \frac{\partial T}{\partial y} + w \cdot \frac{\partial T}{\partial z} \right) \\ = k \cdot \left( \frac{\partial^2 T}{\partial x^2} + \frac{\partial^2 T}{\partial y^2} + \frac{\partial^2 T}{\partial z^2} \right) + q \end{aligned} \tag{6}$$

**Table 3** Parameters of the heat fin

Case study no.	Factor	Range
1	Fin height	9–22 mm
2	Number of perforations	1–7
3	Perforation major axis length	1–5 mm
4	Perforation minor axis length	1–2.5 mm
5	Number of fins	3–15

where  $q$  is the volumetric heat source,  $k$  is the thermal conductivity, and  $\nu$  is the kinematic viscosity of air. Table 3 summarizes the details of analysis performed in the present work. Figure 2 shows the design of fin adopted in this analysis.

### 3 Heat Transfer Analysis: Results of Numerical Simulation

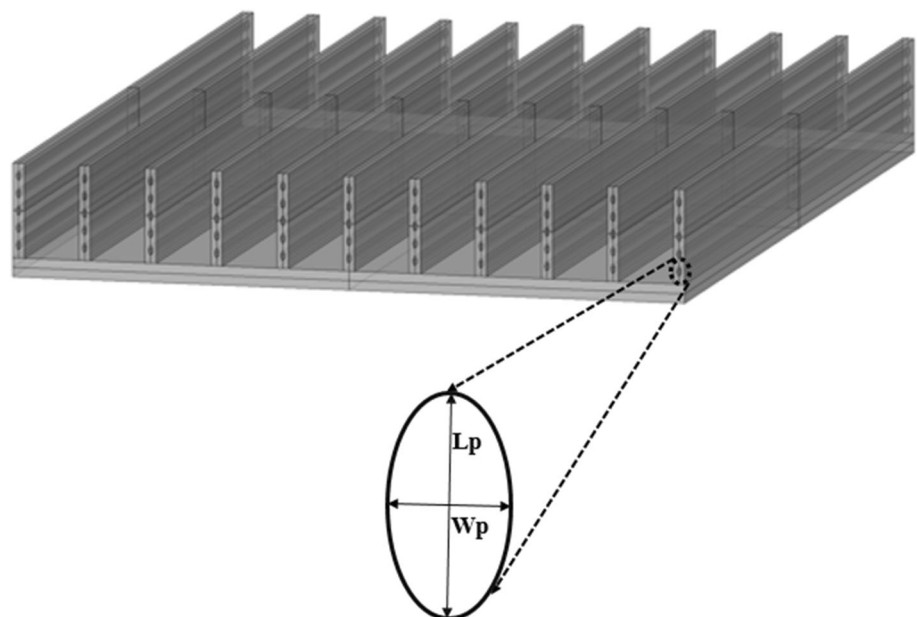
In the following sections, the effect of heat sink geometric parameters on the base plate temperature is analyzed. The perforated model is compared with the conventional solid fin. In the graphs, the zero value of the number of perforations and perforation dimensions indicates solid fins. The effect of fin height, the number of perforations, perforation geometry and spacing of the perforations on the base plate temperature is studied.

Increasing the fin height facilitates an additional volume of fresh air to make contact with the fin area, thereby increasing the total heat transfer rate and velocity of air. When there is an increase in fin height, there is an increase in heat transfer rate. By introducing elliptical perforation, more air will flow over on the fin resulting in enhanced heat transfer rate. The increase in the number of perforations, on the one hand, increases the heat transfer rate by allowing the convective fluid to flow through the perforations. On the other hand, it also reduces the conductive heat transfer. This causes an optimality condition for enhanced heat transfer. The effect of perforation on the base plate temperature is a combined role of convective heat transfer and conduction heat transfer. As the number of perforations

increases from 1 to 5 in Fig. 3, the increased convective heat transfer plays an important role. This leads to the reduction in base plate temperature as more heat is carried away by the convective fluid. However, with a further increase in the number of perforations (above 5), the base plate temperature starts to increase. This shows that there is a reduced conduction heat transfer as a result of an increased loss of solid fin volume which overrides the increased convection, leading to increasing temperature as shown in Fig. 3. The characteristic of an elliptical perforation is determined by its major and minor axes. With the increase in the dimension of the elliptical perforation, the flow rate of air through the perforation increases, thus increasing the effective heat transfer coefficient and decreasing the base plate temperature. Fin spacing also plays a vital role in the heat transfer. It is found that as the fin spacing decreases, the heat transfer rate is enhanced, leading to the decrease in base plate temperature. However, having more fins on the base plate results in less fin spacing which further results in less space available for air flow. Thus, the heat transfer rate decreases when the fin spacing is much less in the case of a base plate with more fins. The temperature variation of the base plate corresponding to the above-mentioned conditions is represented in Fig. 3.

Another important feature of the perforated fin is the weight reduction in fins when compared to conventional solid plate fins. This is of pronounced importance in many manufacturing and aero-industries. Key contemplation in the field of manufacturing is related to material costs. A potential weight reduction of up to 72% is obtained by the introduction of elliptical longitudinal perforation in the present work. Volume reduction is calculated using Eq. 7.

**Fig. 2** Horizontal view of elliptically perforated fin with dimensions



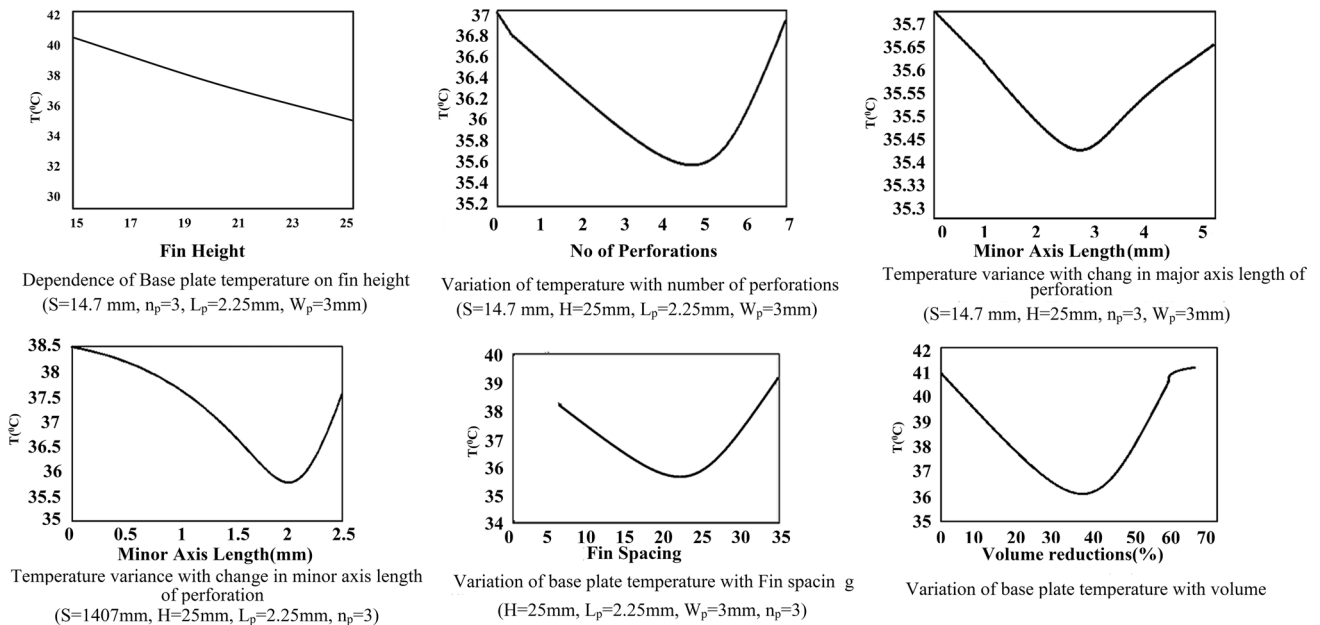


Fig. 3 Variation of base plate temperature

$$\text{Volume reduction(\%)} = \frac{\text{Area of ellipse} \times \text{length of the perforation} \times \text{number of perforations}}{\text{volume of solid fin}} \quad (7)$$

The parameters for the maximum weight reduction obtained are shown in Table 4. It can be observed from Table 4 that this parameter set does not correspond to that with the highest augmentation rate. This is also clear from Fig. 3.

### 4 Proposed Optimization Method

There is a need to find a holistic or multiobjective optimum to achieve a good design of fins with elliptical perforation. In few cases, fins that had contributed to high weight reduction caused a decrease in heat transfer when compared to the fin structure without perforation. Optimization algorithm requires objective functions. One objective function is to maximize the LHS of Eq. 7. Obviously, the second objective is to minimize the base plate temperature or to maximize the Nusselt number. A relation needs to be established between the fin parameters and the Nusselt number. In general, multiple regressions are used to arrive at the objective functions. In this case, we have more than one objective function. The artificial neural network is a learning-based prediction technique that is widely used in the determination of dependent variables in heat transfer problem. One such method was demonstrated by the authors in Balachandar et al. (2015). The objective function predicted using artificial neural network was later

Table 4 Parameters for maximum weight reduction

Parameter	Optimal value
Fin height	25 mm
Number of perforations	7
Perforation major axis length	2.6 mm
Perforation minor axis length	2.93 mm
Number of fins	13
Weight reduction	72%
Temperature increase or decrease compared to conventional fin	Increase (5%)

optimized using a genetic algorithm (GA). GA is an optimization tool based on the evolution of organisms—survival of the fittest. The genetic algorithm provides a way for multiobjective optimizations (Balachandar et al. 2015). The formulation of GA for a multiobjective optimization is quite difficult and tedious. Hence, there is a requirement of a hybrid optimization method to obtain the multiple response optimizations for the design of fins with elliptic perforations.

MANFIS is an extension of general adaptive neuro-fuzzy inference system. It models the relationship between the dependent and independent variables without referencing any prespecified mathematical functions. MANFIS structure can be regarded as a combination of many independent ANFIS systems (Culliere et al. 1995). In this study, MANFIS and GA have been integrated together to

find the optimal fin parameters for augmented heat transfer and with minimum weight.

### 4.1 Nusselt Number Prediction Using Nonlinear Relation

It can be envisaged from the heat transfer analysis in the preceding section that the base plate temperature depends on various parameters associated with the fin geometry. In order to estimate the heat transfer rate or the non-dimensional Nusselt number, multiple regressions are to be used. The change in heat transfer coefficient is obtained when perforations are introduced in the solid fin. In all the cases the convective heat transfer coefficient at the perforated surface increased. However, the overall heat transfer coefficient changed as a result of a change in effective conduction in addition to the convective coefficient. The heat transfer coefficient for the perforated fins is obtained by the calculation of the heat flux (from the constant heat source) considering the difference between the predicted base plate temperature and the ambient.

The predicted Nusselt number equation is shown in Eq. 8. These values are obtained based on the consideration of 300 simulations taken from the entire 1024 set of simulations done in the present analysis.

$$Nu = 2.892 \left(\frac{s}{L}\right)^{-0.0664} \left(\frac{H}{W}\right)^{-0.31} Ra^{0.248} P^a, \tag{8}$$

where  $a = 0.2280$  for  $P \leq 5.511 \times 10^{-4}$   
 $-1.154$  for  $P > 5.511 \times 10^{-4}$   
 and  $P = \frac{L_p W_p n}{LW}$ . (9)

In order to check the effectiveness of the correlation given in Eq. 8, a regression plot is plotted as shown in Fig. 4 with large deviating values. It can be seen that regression coefficient for Eq. 8 is around 0.68, which indicates an inefficient prediction-based correlation. Such a poor prediction may lead to inaccurate optimized value when an evolutionary optimization algorithm is used. The poor prediction of the mathematical regression can be highlighted based on the fact that the dependence of the base plate temperature or Nusselt number on the independent parameter is highly nonlinear. Determination of multiple nonlinear regressions is a herculean task, and it is most likely that the regression yields poor prediction. Thus, to predict the Nusselt number value more accurate soft computing methods are used in the present work.

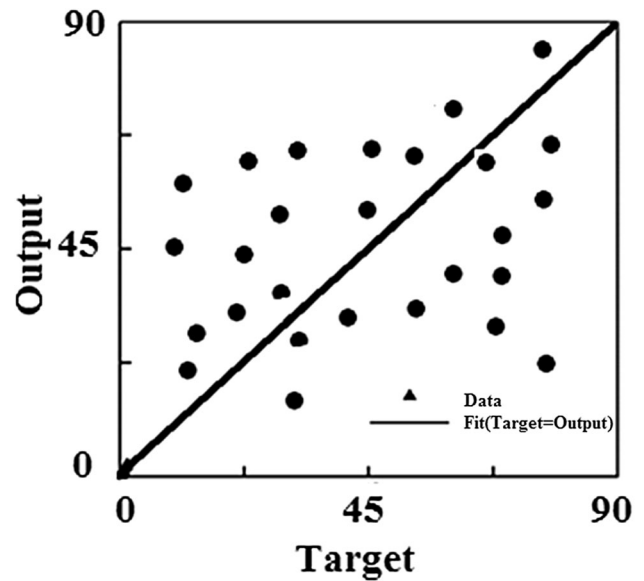


Fig. 4 Regression plot for value predicted from correlation

### 4.2 MANFIS

As discussed earlier, to predict the responses of various combinations of parameters multiple adaptive neuro-fuzzy system is used in the present work. The structure of the MANFIS structure used in present work is shown in Fig. 5.

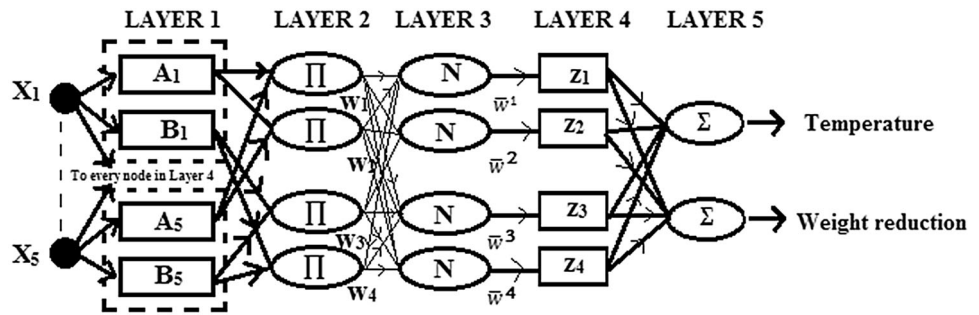
MANFIS structure comprises a network of 5 layers apart from the input layer. In the present work, the dependence of heat transfer on 5 different parameters is evaluated. Hence these 5 parameters are the 5 input nodes. Layer 1 comprises 5 subgroups each with 2 nodes. Each subgroup is connected to an input node. The output of each node in Layer 1 is defined by a membership function on the value of the input. In the present work, a Gaussian function is used. To have better clarity, the output from first node A in the subgroup 1 of Layer 1 is of the form shown in Eq. 10.

$$f_{A1}(x_1) = \exp\left[-\frac{x_1 - v_1}{\sigma_1}\right]. \tag{10}$$

Here  $x_1$  is the input parameter.  $v_1$  and  $\sigma_1$  are the premise parameters. The Gaussian function is multiplied by a weight which is adaptive and is changed in the training process. Nodes in Layer 2 are conjunction operators. They multiply the incoming signals from Layer 1, thus synthesizing the information from the previous layer. The output from the  $j$  node which is obtained as firing strength from  $w_j$  nodes in Layer 3 performs the normalization of the values obtained from Layer 2. The normalized value of  $j$ th node is shown in Eq. 11.

$$\bar{w}_k = \frac{W_k}{\sum_{j=1}^5 W_j}. \tag{11}$$

Fig. 5 Structure of MANFIS used



Layer 4 performs linear combination of the input values and is multiplied by some constants. These constants are also adaptive and are adjusted in the course of network training. These constants are called consequence parameters. The linear combination is multiplied by the value  $\bar{w}_k$  obtained from Layer 3. Layer 5 computes the overall output as a summation of all incoming signals coming from Layer 4. This is the final output. Nonlinear mapping between the independent variable  $x$  and multiple response  $y_i, i = 1, \dots, m$ , is done through MANFIS. The MANFIS is a system which is made to learn with the objective of minimizing the mean squared error between the two outputs. The learning process of premise parameters is accomplished with backpropagation algorithm. Least square approach is used for the learning of consequence parameters. Initially, to ascertain the prediction capabilities of the system, the output nodes are base plate temperature and weight reduction. Total set of data used for training involves results obtained from 300 simulations. The number of epochs is varied until convergence is obtained to ensure optimal training. Output  $y_1$  required around 30 epochs and  $y_2$  required 10 epochs to arrive at a convergent solution. The number of epochs for output  $y_2$  (weight reduction) is less, pertaining to the linear nature of its dependence on fin parameters.

Regression plot between the actual and predicted value is plotted in Fig. 6. The 1024 solution set used to test the prediction rate of regression analysis is used with ANFIS network. A regression coefficient of 0.96 is obtained in comparison with 0.68 obtained using multiple mathematical regression. This ascertains that the prediction capabilities of ANFIS are phenomenally higher than that of multiple regression.

### 4.3 MANFIS–GA Optimization

MANFIS–GA optimization is based on the Zimmerman’s max–min approach (Zimmermann 1978). Now the output vector of MANFIS system has two quantities. One is the temperature of the base plate, and the other is weight reduction. The present objective is to obtain a holistic set of

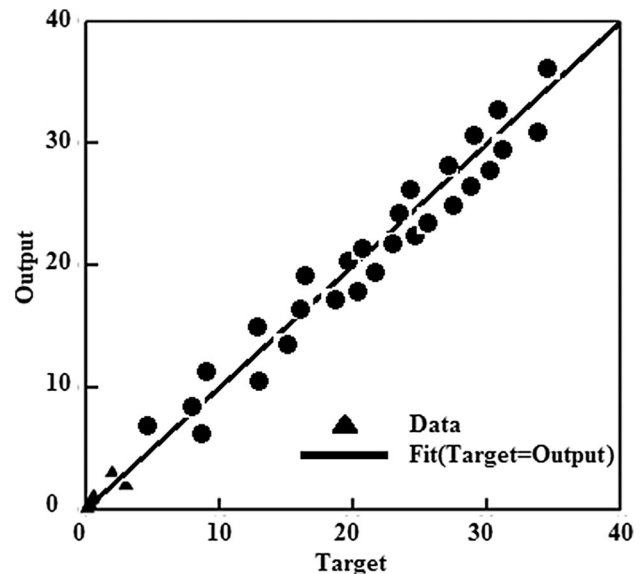


Fig. 6 Regression plot (only large deviation values are shown)

parameters that will give the best result considering both temperature and weight reduction. Thus, the objective functions are to minimize the base plate temperature and maximize weight reduction. A slight modification is done in the ANFIS structure in which a membership function is formulated for each output node. Maximizing the weight reduction comes under the category “the larger the better” as presented in Zimmermann (1978), whereas minimizing the base plate temperature comes under the category “the smaller the better.” According to the approach in Zimmermann (1978), an overall satisfactory optimal value can be obtained with the use of membership function among all the responses. The degree of satisfaction of each objective is represented as a membership function  $\phi(i_i)$ , where  $y_i$  is the estimated responses of MANFIS. The membership function for the objective of minimizing the base plate temperature is shown in Eq. 12.

$$\phi(y_1) = \begin{cases} 1, & \text{if } y_1 < y_{\min} \\ \frac{y_{\max} - y_1}{y_{\max} - y_{\min}}, & \text{if } y_{\min} \leq y_1 \leq y_{\max} \\ 0 & \text{if } y_{\max} < y_1 \end{cases} \quad (12)$$



**Table 5** Optimized value

Parameter	Optimal value
Fin height	22 mm
Number of perforations	5
Perforation major axis length	3.5 mm
Perforation minor axis length	2.23 mm
Number of fins	13

**Table 6** Optimized non-dimensional value for 5 no. of perforations

Perforation length (major axis)/fin height	0.16
Perforation width/fin width	0.77
Total volume of perforation/total fin volume	0.86
Total surface area/fin surface area	1.001

The membership function for the objective of maximizing the weight reduction is just the reverse of Eq. 13.

$$\phi(y_2) = \begin{cases} 1, & \text{if } y_2 > y_{\max} \\ \frac{y_1 - y_{\min}}{y_{\max} - y_{\min}}, & \text{if } y_{\min} \leq y_1 \leq y_{\max} \\ 0 & \text{if } y_{\min} > y_1 \end{cases} \quad (13)$$

Now in the modified MANFIS used for optimization, the output nodes which are previously base plate temperature and amount of weight reduction are now replaced by the membership functions  $\phi(y_1)$  and  $\phi(y_2)$ . Since the objective function is now in the form of the membership function, simple optimization methods cannot be used. Evolutionary optimization techniques such as genetic algorithms are the easier means to evaluate an accurate answer. The optimization problem can be formulated as a minimization problem.

In the present MANFIS–GA algorithm the minimization function forms the fitness function. GA encodes each data point in the set of all solutions as a set of binary digits called chromosomes. A chromosome length of 220 is used with the same number of initial population. Rank selection operator is used for crossover probability of 0.9 and mutation probability of 0.2. The use of high crossover probability is to retain the higher fitness obtained in the previous generations. Mutation creates new chromosomes which are subtly different from the current generation.

Therefore, it can provide a new search direction and prevent the population from converging to a local optimum early. However, in the present case, such chances are quite high as the system is highly nonlinear. Hence, a mutation probability of 0.2 is used. Thus, in GA, chromosomes evolve based on selection, crossover and mutation till the convergence of the optimal value is reached.

#### 4.4 Optimization Results and Comparison

The solver is run until convergence, and optimal parameters are determined as mentioned in Table 5. The physical significance of these optimal values can be understood based on the discussion in Sect. 3. The optimal values are converted into non-dimensional values as represented in Table 6. The obtained optimal parameters are numerically modeled, and the simulation is run to determine the temperature. The obtained optimal values are found to enhance the heat transfer by 19.25% when compared to the solid fins of same dimensions. The design is also found to reduce the weight of the heat sink by 63% when compared to the conventional heat sink. The obtained heat transfer enhancement and weight reduction corresponding to optimal parameters determined using the MANFIS–GA and multiple regression presented in the present work are compared and are shown in Table 7.

It should be noted that the values presented in Table 6 are obtained after performing the numerical simulation for the optimal values determined by the tested algorithms. It can be seen that MANFIS–GA provides better results in terms of both the objectives for elliptical perforations. It should be recalled that the motivation of the present work was to implement a method which searches in a more intelligent way to bring out the best set of parameters. Different methods bring out different optimal parameters. However, the aim here is to bring out the best set of optimal parameters that brings out maximum heat transfer enhancement as well as weight reduction. The hybrid MANFIS–GA algorithm achieves this when compared to the multiple regression because of the better selection technique the latter uses. The optimized elliptical perforation is found to provide an enhanced heat transfer rate and weight reduction when compared to conventional solid fins and has a wide industrial application. Overall, the effect of introducing perforations is to enhance the heat transfer from the heated plate. The increase in the number of perforations tends to increase heat transfer rate by increase in

**Table 7** Comparison of results

Objective	MANFIS–GA (%)	Multiple regression (%)
Heat transfer enhancement (compared to solid fins)	19.25	7.25
Weight reduction compared to solid fins	63.2	44

convection by the fluid (air). However, this concession with the decrease in heat transfer is due to reduced conduction. The algorithm determines the optimal number of perforations to achieve the highest heat transfer rate beyond which the effect of increasing the number of perforations on the enhancement of heat transfer is found to be detrimental. Similarly, considering this combined effect of convective heat transfer of air and the conduction due to the wall, optimal parameters for fin spacing and the dimensions of the perforations are determined. In this case, for dimensions that deviate from the determined optimal values, the overall performance of the heat fin is found to decrease. Thus, the presented technique provides the set of optimal parameters from the input set to arrive at the dimensions for a heat sink with enhanced overall heat transfer performance (efficiency) and an overall reduction in weight.

## 5 Conclusion

In this paper, numerical simulation of elliptically perforated fins is done using commercial CFD code. Initially, the model is validated with the available experimental results. This is followed by a parametric study with variations in the number of perforations, perforation dimensions, fin height and the number of fins. Post-processing results showed that there is an optimal value of perforation dimensions, the number of perforations and the number of fins to achieve the maximum heat transfer. Moreover, the introduction of elliptical perforations leads to considerable weight reduction in the fin. MANFIS–GA system is used to arrive at the optimized design of elliptical perforations keeping the minimum base plate temperature and the maximum weight reduction as the primary objective. The algorithm is found to accurately choose the best design parameters for elliptically perforated fins to provide an augmented heat transfer with weight reduction when compared to a solid fin. The algorithm chooses the best design according to the given set of input parameters. The fin designed using the algorithm can replace the existing conventional fins in many applications that require weight reduction of heat sink assembly in addition to heat transfer augmentation.

## References

- Alessa AH, Al-Hussien FMS (2004) The effect of orientation of square perforations on the heat transfer enhancement from a fin subjected to natural convection. *Heat Mass Transfer* 40:509–515
- Akyol Ugur, Bilen Kadir (2006) Heat transfer and thermal performance analysis of a surface with hollow rectangular fins. *Appl Therm Eng* 26:209–216
- Al Essa AH, Al-Odat MQ (2009) Enhancement of natural Convection heat transfer from a fin by triangular perforations of bases parallel and toward its base. *Arb J Sci En* 34(2B):531–544
- Al Essa AH, Al-Widyan MI (2008) Enhancement of natural convection heat transfer from a fin by triangular perforations of bases parallel and toward its tip. *Appl Math Mech* 29(8):1033–1044
- Al Essa AH, Maqableh AM, Ammourah S (2009) Enhancement of natural convection heat transfer from a fin by rectangular perforations with aspect ratio of two. *Int J Phys Sci* 4(10):540–547
- Al-Essa AH (2012) Augmentation of heat transfer of a fin by rectangular perforations with aspect ratio of three. *Int J Mech Appl* 2(1):7–11
- ANSYS (2008) *Fluent 12.0 User's manual*, ANSYS, Inc.
- Balachandar C, Arunkumar S, Venkatesan M (2015) Computational heat transfer analysis and combined ANN–GA optimization of hollow cylindrical pin fin on a vertical base plate. *Sadhana* 40(6):1845–1863
- Çakar KM (2009) Numerical investigation of natural convection from vertical plate finned heat sinks. M.S. Thesis, Middle East Technical University, Ankara
- Chambers JM (1992) Linear models. In: Chambers JM, Hastie TJ (eds) Chapter 4 of statistical models in S. Wadsworth & Brooks/Cole, Pacific Grove
- Churchill SW, Chu HHS (1975) Correlating equations for laminar and turbulent free convection from a vertical plate. *Int J Heat Mass Transf* 18:1323–1329
- Culliere Th, Titli A, Corrieu JM (1995) Neuro-fuzzy modeling of nonlinear systems for control purposes. *Fuzzy systems*. In: International joint conference of the 4th IEEE international conference on fuzzy systems and the second international fuzzy engineering symposium, Proceedings of 1995 IEEE international, vol 4. IEEE
- Dorignac E, Vullierme JJ, Broussely M, Foulon C, MokkaDEM M (2005) Experimental heat transfer on the windward surface of a perforated flat plate. *Int J Therm Sci* 44:885–893
- Güvenç A, Yüncü H (2001) An experimental investigation on performance of fins on a horizontal base in free convection heat transfer. *Heat Mass Transf* 37(4):409–416
- Huang CH, Liu YC, Ay H (2015) The design of optimum perforation diameters for pin fin array for heat transfer enhancement. *Int J Heat Mass Transf* 84:752–765
- Kutscher CF (1994) Heat exchange effectiveness and pressure drop for air flow through perforated plates with and without crosswind. *J Heat Transfer* 116:391–399
- Leung CW, Probert SD (1987) Natural-convective heat exchanger with vertical rectangular fins and base: design criteria. *IMEchE Proc* 201:365–372
- Leung CW, Probert SD (1989) Thermal effectiveness of short protrusion rectangular, heat exchanger fins. *Appl Energy* 34:1–8
- Leung CW, Probert SD, Shilston MJ (1985) Heat exchanger: optimal separation for vertical rectangular fins protruding from a vertical rectangular base. *Appl Energy* 19:77–85
- McAdams WH (1954) *Heat transmission*. McGraw-Hill, New York
- Prasad BVSSS, Gupta AVSSKS (1998) Note on the performance of an optimal straight rectangular fin with a semicircular cut at the tip. *Heat Transfer Eng* 14(1):53–57
- Sahin Bayram, Demir Alparslan (2008a) Performance analysis of a heat exchanger having perforated square fins. *Appl Therm Eng* 28(5/6):621–623
- Sahin B, Demir A (2008b) Performance analysis of a heat exchanger having perforated square fins. *Appl Therm Eng* 28:621–632
- Shaeri MR, Jen TC (2012) The effects of perforation sizes on laminar heat transfer characteristics of an array of perforated fins. *Energy Convers Manag* 64:328–334

- Shaeri MR, Yaghoubi M, Jafarpur K (2009) Heat transfer analysis of lateral perforated fin heat sinks. *Appl Energy* 86(10):2019–2029
- Souidi N, Bontemps A (2001) Countercurrent gas–liquid flow in plate-fin heat exchangers with plain and perforated fins. *Int J Heat Fluid Flow* 22:450–459
- Sparrow EM, Ortiz Carranco M (1982) Heat transfer coefficient for the upstream face of a perforated plate positioned normal to an oncoming flow. *Int J Heat Mass Transfer* 25(1):127–135
- Tari I, Mehrtash M (2013) Natural convection heat transfer from inclined plate-fin heat sinks. *Int J Heat Mass Transf* 56:574–593
- Welling JR, Wooldridge CV (1965) Free convection heat transfer coefficient from rectangular fin arrays. *J Heat Transfer* 87:439–444
- Wessa P (2015) Multiple regression (v1.0.38) in free statistics software (v1.1.23-r7). Office for Research Development and Education. [http://www.wessa.net/rwasp\\_multipleregression.wasp/](http://www.wessa.net/rwasp_multipleregression.wasp/). Accessed Dec 2015
- Yazicioğlu B, Yüncü H (2007) Optimum fin spacing of rectangular fins on a vertical base in free convection heat transfer. *Heat Mass Transf* 44:11–21
- Zimmermann H-J (1978) Fuzzy programming and linear programming with several objective functions. *Fuzzy Sets Syst* 1(1):45–55